Ca^{2+}-dependent thermal sensitivity of bacterial MreB assemblies

Dávid Szatmári[1] · Dénes Lőrinczy[1]

Abstract

In the bacterial cells, the actin homolog MreB manages the cellular motions and morphology. MreB polymers are important for cell-wall growing and cell shape determination. Fluorescence microscopy studies investigated that in bacterial cells the MreB polymer forms ribbon-like structures that likely helical nearby of the cell wall at the periphery of the cell. As we presented earlier, the thermal motion of the ribbon-like MreB polymers was slowed down by the addition of millimolar Ca^{2+}. The rapid Ca^{2+} depletion, via EGTA treatment, reordered the polymers into extensive sheets in the presence of magnesium, and further treatment with calcium led to fissured monolayer sheets and the dissociation of filaments into web-like structures which attached to the glass surface. The heat denaturation of MreB assemblies, under varying Ca^{2+} concentrations, was investigated by DSC, and the Ca^{2+}-dependent MreB polymer rearrangement rates were assessed by isoperibol calorimetry. Here, we measured Ca^{2+}-dependent thermodynamics of prokaryotic MreB assemblies. Under high ionic strength, the MreB polymers show multiple thermal components around 60 °C and 82 °C, generated by less and more stable structures. MreB polymers with a relatively slow exothermic kinetics turned to be more stable due to adding millimolar Ca^{2+}. However, changing the calcium concentration from micromolar to nanomolar and subsequently recovered it to micromolar initialized endothermic remodeling of MreB assemblies and the majority of them showed higher stability than before the treatment. Presumably, the final cell shape depends on the assembling of MreB polymers and the ionic milieu. Calcium concentration-induced changes of MreB structure makes sense in membrane remodeling during prokaryotic cell division or osmotic adaptation.

Keywords Prokaryotic cytoskeleton · MreB · Isothermal kinetics

Introduction

MreB is the member of a huge family of actin-like prokaryotic proteins, it plays important role in managing the cell-wall growth and function in case of gram-negative and gram-positive bacterial cells. Gram-negative species have a slim peptidoglycan layer with a cytoplasmic and outer membrane, and gram-positive species have a wide peptidoglycan wall out of a cytoplasmic membrane [1, 2]. The first time observed due to microscopy that MreB polymers form helical structure close to the cell wall [3, 4] then figured up that short segments of MreB filaments attach to the cytoplasmic membrane [5–7].

Microscopy and spectroscopy studies interpret the importance of in vitro conditions how divert their supramolecular structure and polymerization of MreB [8, 9]. Millimolar magnesium and high ionic strength are necessary for efficient MreB polymerization. Addition of Ca^{2+} initializes a remarkable change of assemblies what we observe from increases inner strain. Interestingly, reduction then recovery of Ca^{2+} level leads to the dissociation of filaments into web-like structures [9]. In vivo ion conditions keep on the state of short MreB polymers to avoid their stacking [9–12]. MreB polymerization shows some sensitivity to the type of bound nucleotide [8, 13]. Polymerization of MreB is accelerated with increasing Mg^{2+} concentration in the presence of ATP [14], while Ca^{2+} does not have any remarkable influence on the process. However, cytoplasmic Ca^{2+} regulates the cell cycle and movement of cells [15].

Previously, it was shown that MreB protofilaments binding together and form antiparallel twisted filaments [16, 17]. The in vitro assemblies are built up by unpolarized filaments which stacking together side by side. Membrane binding can stabilize the MreB polymers [17] and untwisting their filamentous structure [18]. The in vivo existence of short

✉ Dénes Lőrinczy
   denes.lorinczy@aok.pte.hu

1   Department of Biophysics, Medical School, University
    of Pécs, Szigeti Str. 12, Pecs 7624, Hungary

and rigid polymers can provide a good evidence that the regulation of their flexibility is only based on the length of the filaments. The binding of untwisted MreB filaments may stabilize the curvature of the membrane [18]. The Ca^{2+} concentration-dependent inner strain of MreB polymers can be crucial to determine the bending of cell wall via membrane-MreB interactions [9, 19]. Cell shape seems independent of various ionic conditions; however, they affect membrane dynamics and enzyme activity, which effects the MreB system and stability of bacterial cell wall [20]. Interestingly, the cell size and cell cycle are possibly regulated by Ca^{2+} concentration.

The role of Ca^{2+} ions in the structure and function of MreB filaments are remaining as important questions. It is need more investigation that which ionic conditions are required for the MreB polymers stability, mobility within their assembling and disassembling, how does Ca^{2+} ion concentration affects these processes. We applied DSC denaturation and isoperibol scans to study the heat response dynamics and rearrangement kinetics of *E.coli* MreB polymers within the change of Ca^{2+} concentration.

Materials and methods

Expression of MreB

The *Escherichia coli* MreB (AJF45056.1) was expressed in *E. coli* BL21 DE3 pLysS strain (Novagen) cells, pSY5 plasmid was applied which encodes a histidine tag. Cell cultures were grown in Luria Broth medium at 37 °C in the presence of ampicillin. The optical density at 600 nm of the culture was reaching 0.6 then followed by protein expression it was induced by 1 mM IPTG overnight at 20 °C. Cells were harvested then stored at −20 °C [21].

Purification of MreB

We used our previously applied polymer filtration (PF) method [9] for the isolation of MreB polymers. *E. coli* cell pellets were homogenized in polymerizing buffer (4 mM MOPS, 300 mM KCl, 2 mM $MgCl_2$, 0.1 mM $CaCl_2$, 0.2 mM ATP, 1 mM MEA, pH 8.0). The slurry was incubated in the presence of DNase (0.01 U mL^{-1}, PanReac, AppliChem) and lysozyme (0.01 mg mL^{-1}, Sigma-Aldrich) overnight at 4 °C. MreB polymers were filtered by the consecutive steps of paper filter then 0.45 μm membrane filter. We did SDS-PAGE to obtain the purity of MreB stocks. The prepared MreB solutions were stored on ice until further application. We measured the concentration of MreB solutions by Bradford Assay (Bio-Rad) and Jasco v-660 photometer (Jasco Corporation).

Fluorescent labeling of MreB

Alexa Fluor 488 C5 maleimide was applied for labeling the cysteine of MreB. DTT was removed from the solution by overnight dialysis prior to initiating of the labeling reaction followed by an incubation step of MreB polymers in the presence of fivefold molar excess of the fluorophore for 1 h on ice. Then, applied excess fluorophore was removed by overnight dialysis to remove the excess fluorophore from the solution. We used spectrophotometry ($\varepsilon_{Alexa488} = 73{,}000$ M^{-1} cm^{-1}, $\varepsilon_{EcMreB} = 7575$ M^{-1} cm^{-1}) to determine the concentrations of protein and fluorophore in the samples. Then, calculated the labeling ratio as the concentration ratio of the probe to the protein and was found to be approximately 10% in cases of MreB polymers.

Fluorescence microscopy

The morphologies of the Alexa488-MreB polymers were visualized by Leica TCS SP confocal scanning microscope system (Leica Microsystems GmbH Germany) equipped with a 10-63X objective lens. Prior to the microscopy 15 μL of sample was dropped on slides, incubated in the presence of the indicated buffer, then covered by coverslips. Image acquisition was carried out a fluorescent-probe specific wavelengths, Alexa488 (ex.: 488 nm, em.: 515–560 nm). The typical vertical stacking height of images was 1–3 μm.

DSC measurements

We applied SETARAM Micro-DSCII calorimeter on room temperature, 22 °C for 6 h to investigate isotherm kinetics analysis. Hastelloy designed pair of "mixing batch" vessels were applied for isoperibol measurements ($V_{lower} = 500$ μL, $V_{upper} = 200$ μL) in the reference vessel the MreB was mixed with buffer or EGTA contained buffer and in the sample one with Ca^{2+} to provide the different final Ca^{2+} concentrations (calculated by MaxChelator, https://somapp.ucdmc.ucdavis.edu). After the first hour of measurement, we observed the continuous approaching of heat flow to zero which can be described by the decay of ATP. The first point of our analysis was the initial point of the heat flow change ($\Delta Q_{initial}$) after a single sharp peak which shows the mixing effect, and thus the curve was changed slowly to the top point (ΔQ_{top} see Fig. 3B). The measurements were started in 5 min after reaching the thermal equilibrium between the vessels then the exponential fitting resulted the time rate (k) of the peaks. We used for the analysis the part of the curve after the mixing

effect. MreB and Ca^{2+}-based molecular events were happened only in the first hour thus the most reasonable time duration of kinetics was analyzed in the first 3000 s.

Denaturation heat measurements were carried out by heating up the samples with 0.3 K min^{-1} between 40 and 80 °C. The reference was only MOPS buffer. The equilibrated mass precision was ± 0.1 mg between the reference and sample vessels therefore their heat capacity difference was not applicable. With the help of a two-point SETA-RAM peak integration setting, the denaturation calorimetric enthalpy was calculated from the area under the heat absorption curve, and then, the results [denaturation or melting temperature (T_m) and calorimetric enthalpy (ΔH_{cal}) data of samples] were compared. This method is identical with the protocol as we applied in our previous studies [22–24].
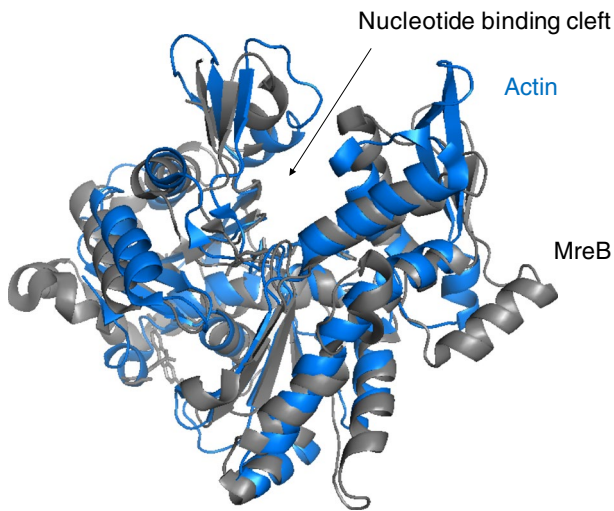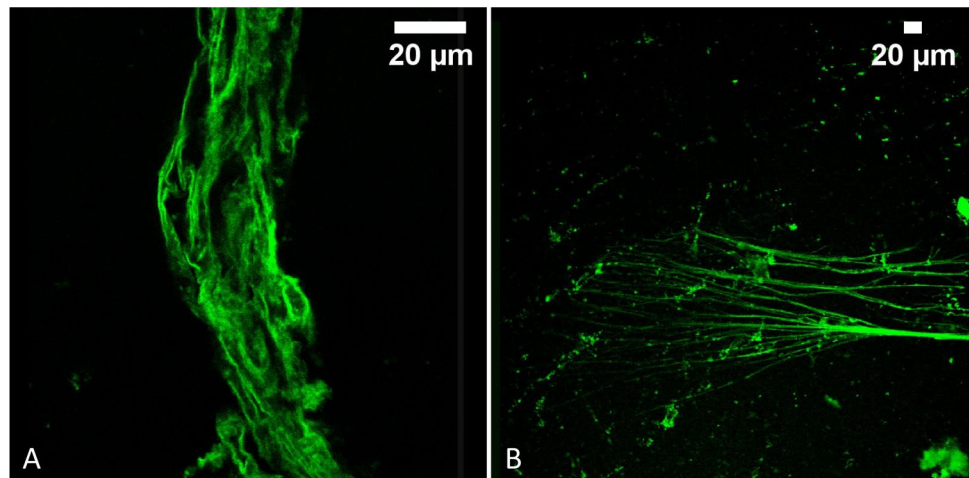

Fig. 1 MreB is a prokaryotic actin homolog. *E.coli* MreB and human actin monomers show 90% structural identity, both can bind nucleotides and capable to do polymerization. PDB: MreB 1JCE, actin 2HF4

Results

Figure 1 shows structural similarity between the eukaryotic actin and the prokaryotic MreB. However, the structural identity of monomers is around 90% their polymers show major differences in structural, dynamical and kinetical properties.

As we determined previously, bacterial cells intracellular ionic strength is relatively high [9]. Therefore, MreB forms huge superstructures under polymerizing conditions (300 mM KCl, 0.2 mM ATP, 2 mM MgCl$_2$) [21] in the presence of 0.1 mM CaCl$_2$ (Fig. 2A), while under the same conditions, actin reaches the highest organization level in filamentous stage [25–27]. Reduction then subsequent recovery of Ca^{2+} concentration in the range of nanomolar to micromolar is remodeling MreB assemblies to extended sheets and web-like structures attaching to the glass surface [9] (Fig. 2B), in case of actin the change of Ca^{2+} concentration only disturbs the steady-state dynamics of filaments [28].

We performed thermal denaturation with heating rate of 0.3 K min^{-1} (Fig. 3A). Multiple local maxima were observable in case of MreB in the presence of micromolar Ca^{2+}, indicated peaks in lower range at 57 and 61 °C, and in peaks of higher range at 79, 82, 87 as well as 90 °C (see Table 1), the total enthalpy change was distributed equally between two ranges 0.3 ± 0.05 J g^{-1} and 0.3 ± 0.03 J g^{-1}, respectively. MreB polymers after the addition of millimolar Ca^{2+} responded with three maxima in lower range at 55, 57 and 60 °C, and with six maxima in the higher range at 68, 71, 74, 79, 87 as well as 92 °C (see Table 1), the enthalpy change was three times larger in the higher range 0.4 ± 0.01 J g^{-1} than in the lower range 0.13 ± 0.03 J g^{-1}. After the reduction of Ca^{2+} concentration from micromolar to nanomolar then its subsequent recovery to micromolar caused the rearrangement of MreB polymers and a more defined response (0.49 ± 0.04 J g^{-1}) in the higher range with

Fig. 2 Ca^{2+}-sensitive rearrangement of MreB polymers. Confocal fluorescent microscopy imaging of Alexa488-MreB **A** under polymerizing conditions 300 mM KCl, 0.2 mM ATP, 2 mM MgCl$_2$ in the presence of 0.1 mM CaCl$_2$, **B** polymers were transformed to sheets and web-like structures due to 2 mM EGTA then subsequently applied 2 mM CaCl$_2$

Fig. 3 Ca^{2+}-dependent rearrangement of MreB polymers. **A** DSC scans, the lines are the average of three independent measurements. Heat denaturation of MreB polymers in the presence of micromolar Ca^{2+} (black line), in the presence of millimolar Ca^{2+} (purple line), after the reduction of Ca^{2+} concentration from micromolar to nanomolar then recovery to micromolar (orange line). **B** Schematic curve of isothermal heat flow change by the time with the mixing effect and the investigated parameters. **C** Time-dependent change of isoperibol heat flow in case of MreB polymers, due to millimolar Ca^{2+} addition (purple line), or due to the recovery of Ca^{2+} concentration from nanomolar to micromolar (orange line). The endotherm effect is deflected downward. Curves are the average of three independent measurements. (Color figure online)
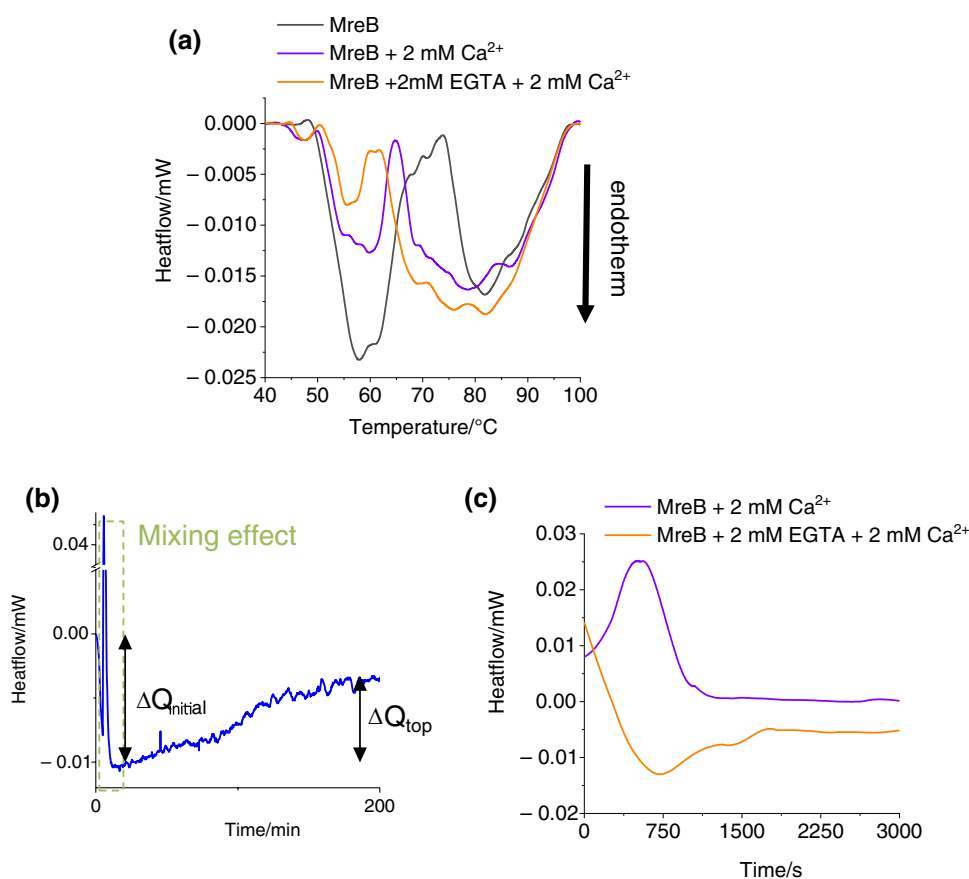

Table 1 Heat denaturation parameters. The values are the average ± SD (in case of temperature differences between 0.2 and 0.5 °C) of three measurements

Ca^{2+} level	Thermal parameters			
	T_m/°C		ΔH_{cal}/J g^{-1}	
	Low range	High range	Low range	High range
μM	57, 61	79, 82, 87, 90	0.3 ± 0.05	0.25 ± 0.03
Changed from μM to mM	55, 57, 60	68, 71, 74, 79, 87, 92	0.13 ± 0.03	0.4 ± 0.04
Changed from nM to μM	55, 57	68, 76, 82	0.05 ± 0.01	0.49 ± 0.05

the local maxima at 68, 76, 82 °C, and a smaller calorimetric enthalpy (0.05 ± 0.01 J g^{-1}) in the lower temperature range at 55 and 57 °C (see Table 1).

For the better understanding of the MreB polymers remodeling due to Ca^{2+} ion fluxes, we carried out isoperibol calorimetry assays. In case of isoperibol measurements the first relevant 3000 s following the mixing effect was important, between the initial ($\Delta Q_{initial}$) and the top points of the heatflow change (ΔQ_{top}) (Fig. 3B). After a single sharp peak (mixing effect), the initial point of the heat flow change was first point of our analysis followed by the curve which was investigated as thermal response of molecular processes (Fig. 3B). The time rate of the peaks was defined by exponential fitting. MreB polymers were reacted to millimolar Ca^{2+} addition with a relatively quick

Table 2 Exponential fitting to the curves between the initial and top value obtained the isothermal kinetic data

Ca^{2+} change	k/*10^{-4} μW s^{-1}	ΔQ_{ini}/μW	ΔQ_{top}/μW
Isotherm kinetic parameters			
μM to mM	49 ± 2	7.7 ± 0.6	25 ± 1.8
nM to μM	12 ± 1	13.7 ± 2	− 13 ± 0.7

The values are the average ± SD of three measurements

(rate of change 49 ± 2 × 10^{-4} μW s^{-1}) exothermic (17.3 μW) response (see Table 2), in the first 660 s the heatflow was increased from 7.7 to 25 μW (Fig. 3C). However, the reduction and a subsequent recovery of Ca^{2+} level induced a slow (12 ± 1 × 10^{-4} μW s^{-1}) endothermic (− 26.7 mW) change

(Fig. 3B and Table 2), in the first 750 s the heatflow was decreased from 13.7 to − 13 μW.

Discussion and conclusions

The in vitro polymerizing conditions in the presence of divalent and hundred millimolar of monovalent cations drive the growing of huge MreB assemblies [9, 21]. MreB forms different structures with a big variety of organization levels [8]. Heat denaturation of polymers responded in two ranges of peaks with multiple local maxima. Low-temperature range means dynamical MreB structures and high-temperature range belongs to the highly stable forms of huge polymers. The sample possibly contains freely moving oligomers, filaments, small sheets and large polymers which can attach to the wall of the DSC vessels. MreB is able to cover the well charged surfaces (e.g., glass or metal) with monolayer sheets [8] and thereby the bundles of ribbon-like polymers can bind to these extended sheets. Addition of calcium resulted a bigger enthalpy change and more local maxima in the higher temperature range. It can be interpreted as a subsequent stacking of free polymers onto the large assemblies on the surface. The disorder of MreB polymers can be reduced by the stacking of multilayer sheets thus it was happened in an exothermic process, and calcium may cause structural change and increased strain in filaments [9]. Subsequent calcium depletion, via EGTA treatment, in the presence of magnesium was altered their structure and a further Ca^{2+} addition induced fissuring sheets and dissociation of filaments into web-like structures, increasing their structural variance through an endothermic process. The extended web-like assemblies attaching to the surface are going to be more stable and highly resistant against heat.

In vivo MreB assemblies can be stabilized by membrane binding [17]. The structure of filaments can allow bending of the MreB sheets, which may stabilize the curvature of a membrane [18]. The prokaryotic cells possibly lack the existence of motorproteins thus the rearrangement of filamentous system can produce mechanical strain and forces. The large-scale change of calcium concentrations nearby of plasma membrane [19] may provide it by a dynamical MreB scaffold which most likely stabilizing and stacking to multilayers due to the increases Ca^{2+} concentration, and the oscillation of Ca^{2+} level may drive the stabilization and reassembling their ribbon-like sheets. The reshaping of bacterial cells in part of the division or osmotic stress responses can be managed by Ca^{2+} level regulated rearrangement of MreB polymers.

Author contributions DS performed rising the problem, sample preparation and handling, data analysis, and manuscript writing. DL was the corresponding author and principal investigator. DSC provided experiments, data analysis, and manuscript writing.

Data availability There are no additional available data to upload.

Declarations

Competing interests The authors declare that they have no known competing financial interests or personal relationships that could have appeared to influence the work reported in this paper.

Consent for publication Copyright form has been uploaded with the manuscript.

References

1. Vollmer W, Seligman SJ. Architecture of peptidoglycan: more data and more models. Trends Microbiol. 2010;18:59–66.
2. White CL, Kitich A, Gober JW. Positioning cell wall synthetic complexes by the bacterial morphogenetic proteins MreB and MreD. Mol Microbiol. 2010;76:616–33.
3. Jones LJF, Carballido-Lopez R, Errington J. Control of cell shape in bacteria: helical, actin-like filaments in *Bacillus subtilis*. Cell. 2001;104:913–22.
4. Vats P, Rothfield L. Duplication and segregation of the actin (MreB) cytoskeleton during the prokaryotic cell cycle. Proc Natl Acad Sci USA. 2007;104:17795–800.
5. Dominguez-Escobar J, Chastanet A, Crevenna AH, Fromion V, Wedlich-Söldner R, Carballido-López R. Processive movement of MreB-associated cell wall biosynthetic complexes in bacteria. Science. 2011;333:225–8.
6. Garner EC, Bernard R, Wang W, Zhuang X, Rudner DZ, Mitchison T. Coupled, circumferential motions of the cell wall synthesis machinery and MreB filaments in *B. subtilis*. Science. 2011;333:222–5.
7. van Teeffelen S, Gitai Z. Rotate into shape: MreB and bacterial morphogenesis. Embo J. 2011;30:4856–7.
8. Popp D, Narita A, Maeda K, Fujisawa T, Ghoshdastider U, Iwasa M, Maéda Y, Robinson RC. Filament structure, organization, and dynamics in MreB sheets. J Biol Chem. 2010;285(21):15858–65.
9. Szatmári D, Sárkány P, Kocsis B, Nagy T, Miseta A, Barkó S, Longauer B, Robinson RC, Nyitrai M. Intracellular ion

concentrations and cation-dependent remodelling of bacterial MreB assemblies. Sci Rep. 2020;10:12002.

10. Figge RM, Divakaruni AV, Gober JW. MreB, the cell shape-determining bacterial actin homologue, co-ordinates cell wall morphogenesis in *Caulobacter crescentus*. Mol Microbiol. 2004;51:1321–32.

11. Madabhushi R, Marians KJ. Actin homolog MreB affects chromosome segregation by regulating topoisomerase IV in *Escherichia coli*. Mol Cell. 2009;33:171–80.

12. Strahl H, Burmann F, Hamoen LW. The actin homologue MreB organizes the bacterial cell membrane. Nat Commun. 2014;5:3442.

13. Nurse P, Marians KJ. Purification and characterization of *Escherichia coli* MreB protein. J Biol Chem. 2013;288:3469–75.

14. Esue O, Cordero M, Wirtz D, Tseng Y. The assembly of MreB, a prokaryotic homolog of actin. J Biol Chem. 2005;280:2628–35.

15. Holland IB, Jones HE, Campbell AK, Jacq A. An assessment of the role of intracellular free Ca^{2+} in *E. coli*. Biochimie. 1999;81:901–7.

16. Colavin A, Hsin J, Huang KC. Effects of polymerization and nucleotide identity on the conformational dynamics of the bacterial actin homolog MreB. Proc Natl Acad Sci USA. 2014;111:3585–90.

17. van den Ent F, Izore T, Bharat TAM, Johnson CM, Lowe J. Bacterial actin MreB forms antiparallel double filaments. Elife. 2014;3: e02634.

18. Shi H, Quint DA, Grason GM, Gopinathan A, Huang KC. Chiral twisting in a bacterial cytoskeletal polymer affects filament size and orientation. Nat Commun. 2020;11:1408.

19. Dominguez DC. Calcium signalling in bacteria. Mol Microbiol. 2004;54:291–7.

20. Brown AD. Aspects of bacterial response to the ionic environment. Bacteriol Rev. 1964;28:296–329.

21. Barkó S, Szatmári D, Bódis E, Türmer K, Ujfalusi Z, Popp D, Robinson RC, Nyitrai M. Large-scale purification and in vitro characterization of the assembly of MreB from *Leptospira interrogans*. BBA Gen Subj. 1860;2016(9):1942–52.

22. Lőrinczy D, Szatmári D. Dose-dependent effect of cyclophosphamide treatment on actin. J Thermal Anal Calorim. 2022;147:10403–9.

23. Szatmári D, Bugyi B, Pintér R, Lőrinczy D. Cyclophosphamide treatment modifies the thermal stability of profilin bound monomeric and leiomodin2 bound filamentous actin. J Therm Anal Calorim. 2023;148:837–44.

24. Szatmári D, Lőrinczy D. Isotherm kinetics of PIP2 bound gelsolin inactivation. J Therm Anal Calorim. 2023;148:5387–94.

25. Doolittle LK, Rosen MK, Padrick SB. Measurement and analysis of in vitro actin polymerization. Methods Mol Biol. 2013;1046:273–93.

26. Galińska-Rakoczy A, Wawro B, Strzelecka-Gołaszewska H. New aspects of the spontaneous polymerization of actin in the presence of salts. J Mol Biol. 2009;387(4):869–82.

27. Ujfalusi-Pozsonyi K, Hild G, Gróf P, Gutay-Tóth Z, Bacsó Z, Nyitrai M. The effects of detergents on the polymerization properties of actin. Cytometry A. 2010;77(5):447–56.

28. Hild G, Bugyi B, Nyitrai M. Conformational dynamics of actin: effectors and implications for biological function. Cytoskeleton. 2010;67(10):609–29.